ELSEVIER

Journal of Materials Processing Technology 80–81 (1998) 642–646

Journal of Materials Processing Technology

Analysis of metal forming process based on meshless method

Jiun-Shyan Chen [a,*], Cristina Maria Oliveira Lima Roque [b], Chunhui Pan [a], Sérgio Tonini Button [b]

[a] Department of Mechanical Engineering and Center for Computer-Aided Design, The University of Iowa, Iowa City, Iowa 52242, USA
[b] Faculty of Mechanical Engineering, State University of Campinas, Campinas, SP, 13083-970, Caixa Postal 6122, Brazil

Abstract

Conventional finite element analysis of metal forming processes often breaks down due to severe mesh distortion. Since 1993, meshless methods have been considerably developed for structural applications. The main feature of these methods is that the domain of the problem is represented by a set of nodes, and a finite element mesh is unnecessary. This new generation of computational methods reduces time-consuming model generation and refinement effort, and it provides a higher rate of convergence than that of the conventional finite element methods. A meshless method based on the reproducing kernel particle method (RKPM) is applied to metal forming analysis. The displacement shape functions are developed from a reproducing kernel approximation that satisfies consistency conditions. The use of smooth shape functions with large support size are particularly effective in dealing with large material distortion in metal forming analysis. In this work, a collocation formulation is used in the boundary integral of the contact constraint equations formulated by a penalty method. Metal forming examples, such as ring compression test and upsetting, are analyzed to demonstrate the performance of the method.

Keywords: Elasto-plasticity; Large deformation; Meshless method; Metal forming; Reproducing kernel particle method

1. Introduction

Forming processes play an important role in metal part manufacturing. Numerical modeling has been applied to simulate forming processes, in order to predict incoming difficulties such as defects in formed parts, improper tool profile, and low tool lifetime. Numerical simulations prior to experimentation minimizes the traditional 'trial and error' iterations. The simulation of metal forming problems involves geometric, material, and contact non-linearities, and thus requires advanced numerical techniques.

The finite element method (FEM), which has been used in these aforementioned applications, presents some limitations when the mesh becomes highly distorted. In order to avoid these problems, an alternative approach, called meshless method, has been developed [1,2]. The meshless method discretizes a continuum body by a finite number of particles (or nodes) and the displacement field is interpolated under these nodes without the aid of an explicit mesh. This characteristic simplifies model refinement procedures, and the use of the smoother shape functions effectively handles large material distortion simulation [1,2].

Many meshless methods have been developed, including the material point method (MPM) [3], the smooth particle hydrodynamics (SPH) [4], the diffuse element method (DEM) [5], the element free Galerkin methods [6], the reproducing kernel particle method (RKPM) [7] which the present work is based upon, the HP Clouds [8], and the partition of unity method (PUM) [9].

Liu et al. [7] proposed a RKPM based on an integral transformation with modified kernel that exactly reproduces polynomials. The study of the convergence properties of this method is presented in [10]. Chen et al. [1,11] extended RKPM to non-linear hyper-elasticity and elasto-plasticity. A material kernel function

* Corresponding author. Fax: +1 319 335 5669; e-mail: jschen@icaen.uiowa.edu

0924-0136/98/$19.00
PII S0924-0136(98)00171-X

that deforms with the material was introduced to assure the stability during large deformations. A transformation method was also developed to prescribe the essential boundary conditions. The numerical studies indicate that the RKPM is more effective in dealing with large structural distortion than the FEM [1,2,11].

In this paper we present the application of RKPM to metal forming problems such as ring compression test and cold upsetting. Comparison with experiments shows that the RKPM is effective for metal forming applications.

2. Reproduction kernel particle method

2.1. Reproduction kernel shape functions

Consider an integral transformation T of a function u

$$v(x)=Tu=\int_{\Omega}\Phi_a(x-s)u(s)\,\mathrm{d}s, \tag{1}$$

where $v(x)$ is the transformation of $u(x)$. If the kernel $\Phi_a(x-s)$ is chosen to be close to $\delta(x-s)$ then $v(x)\rightarrow u(x)$. The kernel function used in this paper is:

$$\Phi_a(x-s)=\frac{1}{a}\phi\left(\frac{x-s}{a}\right) \tag{2a}$$

$$\Phi(z)=$$

$$\begin{cases} 2/3-4(|z|)^2+4(|z|)^3 & \text{for} \quad 0\le|z|\le 1/2 \\ 4/3-4(|z|)+4(|z|)^2-(4/3)(|z|)^3 & \text{for} \quad 1/2\le|z|\le 1 \\ 0 \quad \text{otherwise} & \end{cases} \tag{2b}$$

where $z=(x-s)/a$ and a is the support of the function $\Phi_a(z)$. This estimation is not accurate near the boundaries. Liu et al. [10] corrected the approximation by introducing a modified kernel function $\bar{\Phi}_a$ as follows:

$$u^a(x)=\int_{\Omega}\bar{\Phi}_a(x;x-s)u(s)\,\mathrm{d}s \tag{3}$$

$$\bar{\Phi}_a(x;x-s)=C(x;x-s)\Phi_a(x-s) \tag{4}$$

where $u^a(x)$ is called the reproduced function of $u(x)$ and it exactly reproduces N-th order polynomial.

$C(x;x-s)$ is called the correction function and was developed to impose the completeness requirement, and $H(x-s)$ is a vector of polynomial of order N.

$$C(x;x-s)=\boldsymbol{H}^T(0)\boldsymbol{M}^{-1}(x)\boldsymbol{H}^T(x-s) \tag{5}$$

$$\boldsymbol{H}^T(x-s)=[1,\, x-s,\, (x-s^2),\, \ldots,\, (x-s)^N] \tag{6}$$

Applying the trapezoidal rule to Eq. (3) one gets:

$$u^a(x)\cong\sum_{I=1}^{NP}\bar{\Phi}_a(x;x-x_1)u(x_1)\Delta x_1=\sum_{I=1}^{NP}\Psi_I(x)u_I, \tag{7}$$

$$\begin{aligned}\Psi_I(x)&=\bar{\Phi}_a(x;x-x_1)\Delta x_1\\ &=\boldsymbol{H}^T(0)\boldsymbol{M}^{-1}(x)\boldsymbol{H}(x-x_1)\Phi_a(x-x_1)\Delta x_1\end{aligned} \tag{8}$$

where NP is the total number of particles and Ψ_I's can be interpreted as the shape functions of $u^a(x)$. Since the kernel function Φ_a in Eq. (2b) is $C^2(\Omega_x)$ one can show that Ψ_I is also $C^2(\Omega_x)$. The purpose of discretizing Eq. (3) is to obtain the shape functions, therefore Δx in Eqs. (7) and (8) is set to unity for simplicity. The extension to multi-dimensional RKPM shape function can be found in [1,2].

3. Meshless formulation in elasto-plasticity with contact conditions

Contact conditions are included to handle contact between tools and workpiece. The classical Coulomb law is used to model frictional contact and the penalty method is applied to assure impenetration. The contact traction's t_n and t_t in the normal and tangential directions, respectively, are defined as follows:

$$t_\mathrm{n}=-\alpha_\mathrm{n}g_\mathrm{n} \tag{9}$$

$$t_\mathrm{t}=\begin{cases}-\alpha_\mathrm{t}g_\mathrm{t} \quad \text{if} \quad |\alpha_\mathrm{t}g_\mathrm{t}|\le|\mu_\mathrm{f}t_\mathrm{n}| \quad \text{(stick conditions)}\\ -\mu_\mathrm{f}t_\mathrm{n}\ \operatorname{sgn}(g_\mathrm{t}) \quad \text{otherwise} \quad \text{(slip conditions)}\end{cases} \tag{10}$$

where μ is the coefficient of friction, α_n and α_t are the normal and tangential penalty numbers, and g_n and g_t are normal and tangential gaps between contact surfaces. The variational equation of the problem can be written as:

$$\int_{\Omega_x}\delta u_{i,j}\tau_{i,j}\,\mathrm{d}\Omega-\int_{\Omega_x}\delta u_i b_i\,\mathrm{d}\Omega-\int_{\Gamma_x^{h_i}}\delta u_i h_i\,\mathrm{d}\Gamma + \int_{\Gamma_x^c}(t_\mathrm{n}\delta g_\mathrm{n}+t_\mathrm{t}\delta g_\mathrm{t})\mathrm{d}\Gamma=0 \tag{11}$$

The contact term is integrated by collocation formulation to yield

$$\int_{\Gamma_x^c}(t_\mathrm{n}\delta g_\mathrm{n}+t_\mathrm{t}\delta g_\mathrm{t})\mathrm{d}\Gamma=\sum_A(F_\mathrm{n}\delta g_\mathrm{n}+F_\mathrm{t}\delta g_\mathrm{t})_A \tag{12}$$

where Ω_x is the current domain, $\Gamma_x^{h_i}$ is the current non-contact traction boundary, and Γ_x^c is the contact boundary, τ_{ij} is the Cauchy stress, b_i is the body force, h_i is the non-contact surface traction, F_n and F_t are the nodal normal and tangential contact forces and A is summed over the contact nodes on the deformable body.

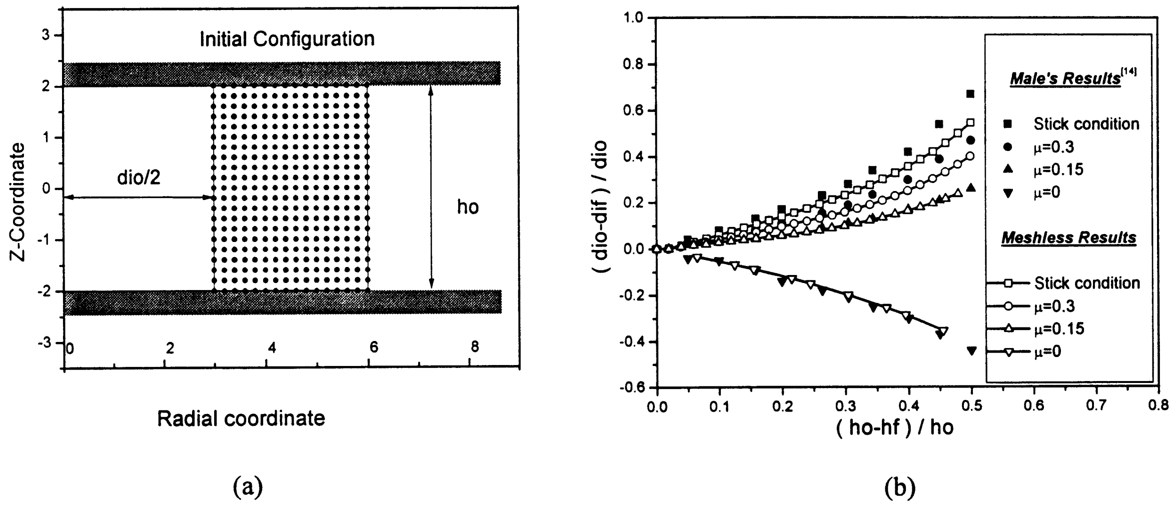

Fig. 1. (a) Ring meshless model, (b) ring calibration curves.

The reproducing kernel shape functions as described in Eqs. (7) and (8) are used in a Galerkin approximation of the variational equation, Eq. (11). The coordinate transformation method [1,2] is used in the discrete RKPM equation so that the contact force F_n and F_t are nodal quantities. The linearization of Eq. (11) leads to a tangential stiffness, and the explicit expression of contact stiffness and contact force in RKPM framework can be found in [11].

The radial return mapping algorithm is used to compute the stress and internal variables [12] and the consistent tangent operator [13], which preserves the quadratic convergence rate of the Newton method, is used. The matrix equations and numerical procedures are given in detail in [1].

4. Numerical examples

Two examples of metal forming processes are modeled: ring compression test and cold upsetting. The ring test was developed to experimentally estimate the friction coefficient in metal forming operations [14]. Upsetting is a basic metal forming operation used in most forging sequences. These analysis are good test problems to verify the use of the meshless method as a simulation and design tool for metal forming applications.

4.1. Ring compression

The test consists of compressing a ring at different ratios with flat and smooth tools and measuring the final height (*hf*) and final internal diameter (*dif*). During compression, the internal and external diameters will change according to the amount of compression and the friction condition of the interface. Hence, curves relating changes in the internal diameter with respect to the compression ratio characterize the coefficient of friction (μ).

The ring test was simulated with physical properties of the cold forging steel 16MnCr5, considered as elastic–perfectly-plastic with yield stress $\bar{\sigma} = 100$ MPa, Young's modulus $E = 288$ GPa, and Poisson's ratio $v = 0.3$. The geometrical dimensions of the ring *deo*:*dio*:*ho* (initial external diameter:initial internal diameter:initial height) are in proportion to 6:3:2. The lubricant used in this test was the bisulfate of molybdenum, which is widely used in cold metal forming processes.

Due to the axial and radial symmetries, the simulation was made with one quarter of the ring (discretized with 160 points). In Fig. 1(a) the half cross section of the initial ring model is shown. The kernel support was chosen to cover five points in each direction and the number of time steps was 1000. The prescribed displacement was applied at the master contact points which simulate the flat tool profile.

The ring test simulation results for coefficients $\mu = 0$ and $\mu = 0.15$ shown in Fig. 1 (b) are in agreement with Male's results [14]. In the case of $\mu = 0.3$ and maximum friction, or stick condition, the results are close to Male's. Kernel functions with supports that cover five and seven points are used to study the solution convergence. Basically, with a bigger support the contact surface appears smoother, but the ring profile remains the same.

4.2. Upsetting

The upsetting process was modeled as shown in Fig. 2(a). In this analysis, axisymmetric formulation

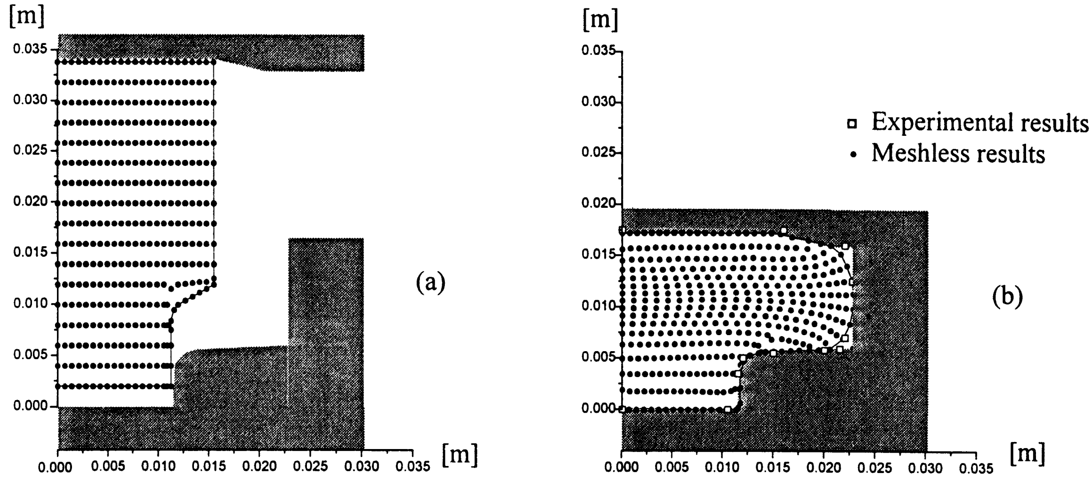

Fig. 2. (a) Initial and (b) deformed configuration of the forging-upsetting operation.

was used, and prescribed displacement was applied to the punch. The material constants are the following: Young's modulus $E = 288000$ MPa, Poisson's ratio $\nu = 0.3$ and the material was considered perfectly plastic with yield stress $\bar{\sigma} = 100$ MPa. Coulomb friction (μ) between punch and part is estimated from experiments, mainly based on lubrication conditions and tools' finishing surface, and is adopted in the model to be equal to 0.15. The final shape is compared to experimental results [15] in Fig. 2(b).

In this analysis, upsetting operation is successfully simulated by the meshless method without experiencing mesh distortion. Numerical prediction of the final shape of the formed part is in good agreement with the experimental results.

5. Conclusions

A meshless formulation based on the RKPM is developed for the metal forming simulation. The emphasis is on the meshless treatment of large plastic deformation and complicated contact conditions. It is shown by numerical examples that the mesh distortion difficulty in the finite element analysis is overcome by the usage of a smooth kernel function with flexibly adjustable support size. The comparison with the experimental data in the ring test and upsetting problem also demonstrated the accuracy of the proposed method.

Acknowledgements

Capes (Fundação Coordenação de Aperfeiçoamento de Pessoal de Nível Superior), a Brazilian funding agency, is greatly acknowledged for the fellowship given to the second author. The support of this research by the National Science Foundation to the University of Iowa is greatly acknowledged.

References

[1] J.S. Chen, C. Pan, C.T. Wu, W.K. Liu, Reproducing Kernel Particle Methods for Large Deformation Analysis of Nonlinear Structures, Comput. Meth. Appl. Mech. Eng. 139 (1996) 195–227.

[2] J.S. Chen, C. Pan, C.T. Wu, Large Deformation Analysis of Rubber based on Reproducing Kernel Particle Method, Comput. Mech. 19 (1997) 211–227.

[3] D. Sulsky, Z. Chen, H.L. Schreyer, A Particle Method for History-Dependent Materials, Comput. Meth. Appl. Mech. Eng. 18 (1994) 179–196.

[4] R.A. Gingold, J.J. Monaghan, Smoothed Particle Hydrodynamics: Theory and Application to Non-Spherical Stars, Mon. Not. R. Astron. Soc. 181 (1977) 375–389.

[5] B. Nayroles, G. Touzot, P. Villon, Generalizing the Finite Element Method: Diffusive Approximation and Diffuse Elements, Comput. Mech. 10 (1992) 307–318.

[6] T. Belytschko, Y.Y. Lu, L. Gu, Element Free Galerkin Methods, Int J. Numer. Methods Eng. 37 (1994) 229–256.

[7] W.K. Liu, Y. Chen, S. Jun, et al., Overview and Applications of the Reproducing Kernel Particle Methods, Arch. Comput. Methods Eng. State Art Rev. 3 (1996) 3–80.

[8] C.A. Duarte, J.T. Oden, An h-p adaptive Method Using Clouds, Comput. Meth. Appl. Mech. Eng. 139 (1996) 237–262.

[9] J.M. Melenk, I. Babuska, The Partition of Unity Finite Element Method: Basic Theory and Applications, Comput. Meth. Appl. Mech. Eng. 139 (1996) 239–316.

[10] W.K. Liu, S. LI, T. Belytschko, Moving Least Square Reproducing Kernel Method (I) Methodology and Convergence, Comput. Meth. Appl. Mech. Eng. 143 (1997) 113–154.

[11] J.S. Chen, C. Pan, C.T. Wu, Application of Reproducing Kernel Particle Methods to Large Deformations and Contact Analysis of Elastomers, Rubber Chem. Technol. 1998 (in press).

[12] R.D. Krieg, S.W. Key, Implementation of a time-independent plasticity theory into structural computer programs, in: J.A.

Stricklin, K.J. Saczalski (Eds.), Constitutive Equations in Viscoplasticity: Computational and Engineering Aspects, AMD-20, ASME, NY, 1976.
[13] J.C. Simo, R.L. Taylor, Consistent Tangent Operators for Rate-Independent Elasto-Plasticity, Comput. Meth. Appl. Mech. Eng. 48 (1985) 101–118.
[14] A.T. Male, M.G. Cockcroft, A Method for the Determination of the Coefficient of Friction of Metals under Conditons of Bulk Plastic Deformation, J. Inst. Met. 93 (1965) 38–46.
[15] C.M.O.L. Roque, Aplicação do Método dos Elementos Finitos no Planejamento da Seqüência de Forjamento a Frio, Master Dissertation, State University of Campinas, Brazil, 1996.